

Electric-field-induced microstructural transformation of carbon nanotubes

Qiaoliang Bao, Han Zhang, and Chunxu Pan^{a)}

Department of Physics, Wuhan University, Wuhan 430072, People's Republic of China
and Key Laboratory of Acoustic and Photonic Materials and Devices of Ministry of Education,
Wuhan University, Wuhan 430072, People's Republic of China

(Received 5 April 2006; accepted 28 May 2006; published online 11 August 2006)

In the present work, microstructural transformation of carbon nanotubes (CNTs) from the “herringbone” into highly crystalline structure in an electric field was experimentally observed by using a high-resolution transmission electron microscope and the growth mechanism was modeled and discussed by using a finite element method. It is found that the CNT microstructures can be changed by an electric field through the influence of the electrostatic force on the carbon surface and bulk diffusion on/in a deformed catalyst particle. Preliminary experiment revealed that an isomeric “graphite-nongraphite-graphite-nongraphite· · ·” CNTs could be synthesized when a pulsed electric field is applied, which are expected to exhibit special properties and promising applications. © 2006 American Institute of Physics. [DOI: 10.1063/1.2227620]

Carbon nanotubes (CNTs) have attracted great interests due to their special microstructure, excellent physical, chemical, and mechanical properties, and promising applications.¹ Generally, variant CNT microstructures determine their properties, for example, highly graphitized CNTs exhibit excellent mechanical and electrical properties;^{2,3} however, the CNTs with defects and poor crystallinity contribute to the field emission property^{4,5} and hydrogen storage capacity.⁶ Therefore, it is of vital importance to control the CNT microstructures effectively for desired applications.

Recently, for the purpose of growing CNTs with different microstructures and crystallinity, many methods have been attempted by changing growth parameters such as catalyst particle size,⁷ growth temperature,⁸ flow rate of carrier gas,⁹ plasma power and bias voltage,¹⁰ etc., in a chemical vapor deposition (CVD) process. Comparing to the regular arc discharge and CVD, flaming and combustion process provides unique advantages for synthesizing CNTs in a simple experiment setup¹¹ and convenience for applying an external electric field, which has been successively used to grow vertically aligned CNTs in our previous research.¹² In addition, it was observed preliminarily that the CNT diameter uniformity and crystallinity of graphite sheets were also improved. In the present work, the mechanism of electric-field-induced CNT microstructural transformation was modeled and discussed and a possible growth of an isomeric “graphite-nongraphite-graphite-nongraphite· · ·” CNT microstructure was proposed which probably exhibits special properties and applications.

The detailed CNT synthesis process by using ethanol flames has been introduced in our previous work.^{11,12} A stainless steel substrate and a Cu biasing electrode at a distance of 50 mm were connected to anode and cathode of a dc power supply, respectively, for generating a uniform electric field parallel to the flaming direction. A power supply was adopted to output dc voltage of 25 V and pulsed rectangular waveguide with the frequency between 0.1 and 5000 Hz. The microstructure and morphology of CNTs were characterized by using scanning electron microscope (SEM, FEI

Sirion, The Netherlands), transmission electron microscope (TEM, JEOL JEM 2010, Japan), and high-resolution transmission electron microscope (HRTEM, JEOL JEM 2010FEF, Japan). The laser Raman spectra were performed in an England Renishaw-1000 laser Raman spectroscopy instrument.

It has been confirmed that the alignment of CNTs became more controllable and repeatable with the assistance of electric field.¹² Figure 1 shows the CNT HRTEM micrographs. It is revealed that (1) CNTs grown without an electric field appeared with a kind of “herringbone structure” which had a larger diameter (32 nm) and more graphite layers (>30) with less-ordered graphitic structure which were inclined to the tube axis ($\approx 20^\circ$), as shown in Figs. 1(a) and 1(b); (2) for CNTs grown in an electric field, the diameter uniformity and the crystallinity of graphite sheets of CNTs were improved clearly, i.e., it exhibited smaller diameter (13 nm) and fewer graphite layers (13–16) parallel to the tube axis, as shown in Figs. 1(c) and 1(d). Laser Raman spectra also verified this microstructural transformation, that is, the CNTs grown in an electric field have smaller I_D/I_G ratio.¹²

Obviously, the electric field played a key role in the above CNT microstructural transformations. Then, it is supposed that an isomeric “graphite-nongraphite-graphite-nongraphite· · ·” CNT microstructure can be synthesized when using a pulsed electric field with variant interpulse intervals. Figure 2 gives the preliminary results regarding a

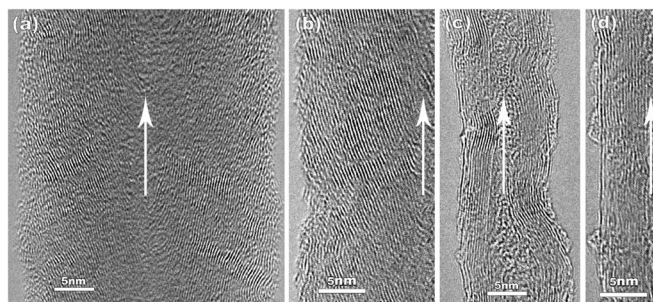


FIG. 1. HRTEM micrographs of CNTs grown [(a) and (b)] without electric field and [(c) and (d)] with electric field. (Arrows indicate the direction of tube axis.)

^{a)} Author to whom correspondence should be addressed; electronic mail: cspan@whu.edu.cn

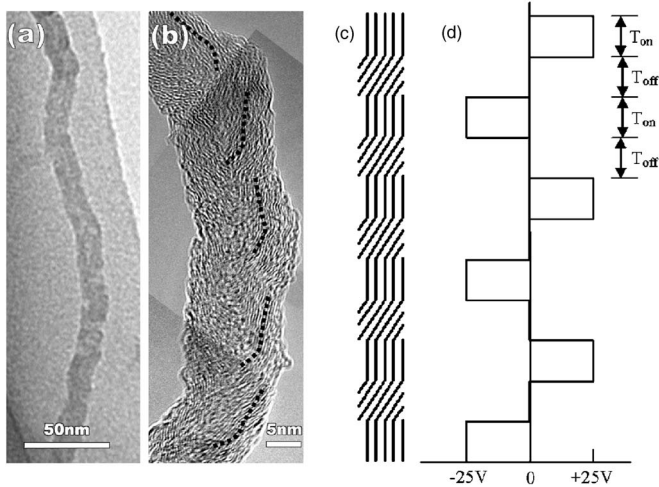


FIG. 2. (a) TEM and (b) HRTEM micrographs of CNTs grown in a 2.5 Hz pulsed electric field, (c) schematic model of graphite layers; (d) pulsed voltage outputted from a power supply.

pulsed rectangular waveguide of power supply with parameter peak voltage of 25 V and a frequency of 2.5 Hz. TEM overall observation shows that there were many defects in the tube wall, as shown in Fig. 2(a). However, further HRTEM examination reveals that the CNT graphite layers varied periodically, almost similar to the voltage cycle from power supply, as shown in Figs. 2(b) and 2(d). Rough calculation indicates that the present isomeric structured CNTs were grown at a rate of about 60 nm/s according to the interpulse interval $T_{on}=T_{off}=100$ ms, which is close to the 50 nm/s result calculated from (Ref. 12), that is, the total CNT length divided by the sampling time. In other words, the time for the CNT to form each segment of the “graphite-nongraphite-graphite-nongraphite...” structure almost matches the electric field cycle.

Figure 3 illustrates the Raman spectra of CNTs grown in pulsed electric field with variant frequencies. The two main peaks D at 1350 cm^{-1} and G at 1600 cm^{-1} were considered. The ratio of the intensity of D peak (I_D) to G peak (I_G) is also used for measuring the amount of disorder in CNTs.^{13,14} It was found that the intensity of disordered D band and the I_D/I_G ratio became larger and larger with frequency increasing, which indicated that the density of disorder graphite layers in tube wall increased at higher frequency. This is because that the less-ordered herringbone structure appears

more frequently with increasing of pulse frequency.

Recently, various mechanisms have been discussed for CNT growth.^{8,15–18} The widely accepted is the diffusion-limited model including three steps: decomposition, diffusion, and precipitation.^{19,20} Obviously, both carbon bulk and surface diffusion in/on a catalyst particle determine the CNT microstructures. Generally, the surface diffusion coefficient upon the particle is much larger than that of the bulk.²¹ Therefore, the particle size and shape play an important role in determining the final CNT graphite structure.²² And to control the CNT microstructure is difficult and complicated.

In the present work, the CNT growth mechanism was supposed to comply with the decomposing-diffusing-precipitating model. The carbon concentration gradient within the undeformed catalyst particle was calculated by numerically solving a steady-state diffusion equation, $J=-D(\partial C/\partial x)$, by using finite element method (FEM) according to Fick’s law. While considering the influence of stress field, the carbon concentration gradient within the deformed catalyst particle was calculated by numerically solving the diffusion equation $\partial c/\partial t=D'(\partial^2 c/\partial x^2)-D''(\partial^2 \varepsilon/\partial x^2)$, where ε is the elastic deformation, the diffusion coefficient D'' represents the flux of uphill diffusion which was only dependent on the stress gradient. It was supposed that the concentration gradient induced diffusion and stress gradient induced diffusion reached equilibrium from the beginning of CNT growth. The boundary conditions were as follows: (1) carbon concentration at the top hemisphere is kept constant at 100 and (2) those at other places are kept zero. The stress and deformation in CNT and catalyst particle were simulated by FEM with the following three hypotheses: (1) CNT wall is an elastic cylinder with Young’s modulus $E_{wall}=4.84$ TPa and Poisson ratio $\nu=0.19$;²³ (2) catalyst particle (Nickel) has Young’s modulus $E_{particle}=0.21$ TPa and Poisson ratio $\nu=0.31$; (3) electrostatic force (500 N/m^2) induced by local electric field ($\sim 4 \times 10^3\text{ V/m}$) (Ref. 12) acts uniformly upon the top hemisphere of the catalyst particle and the bottom of the nanotube is fully constrained.

It is well known that the carbon diffusion in catalyst particle depends upon its stress and deformation states. Preliminary calculation and simulation show that the shape and interior stress states of the particle can be changed by an electrostatic force, which then influences the CNT microstructures, as shown in Fig. 4. In the case of without an electric field, the carbon concentration gradient of bulk dif-

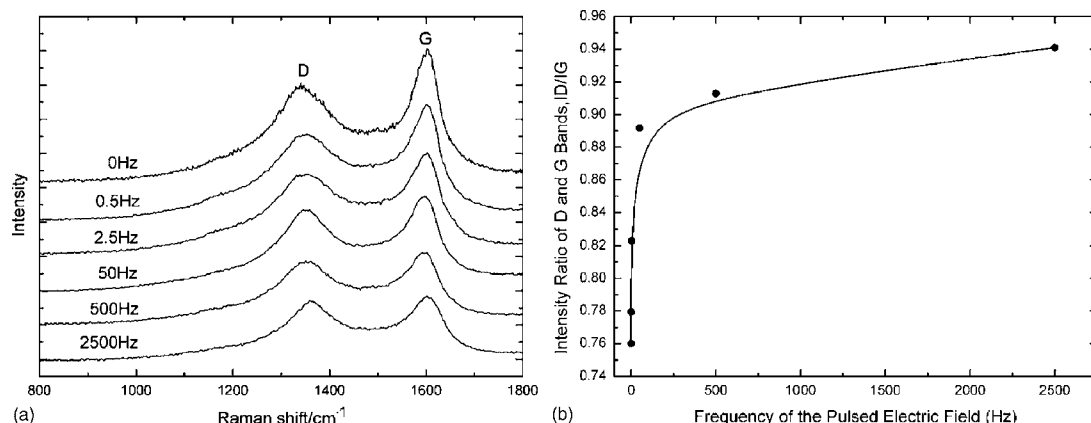


FIG. 3. (a) Raman spectra of CNTs grown in a pulsed electric field with variant frequencies; (b) corresponding I_D/I_G values.

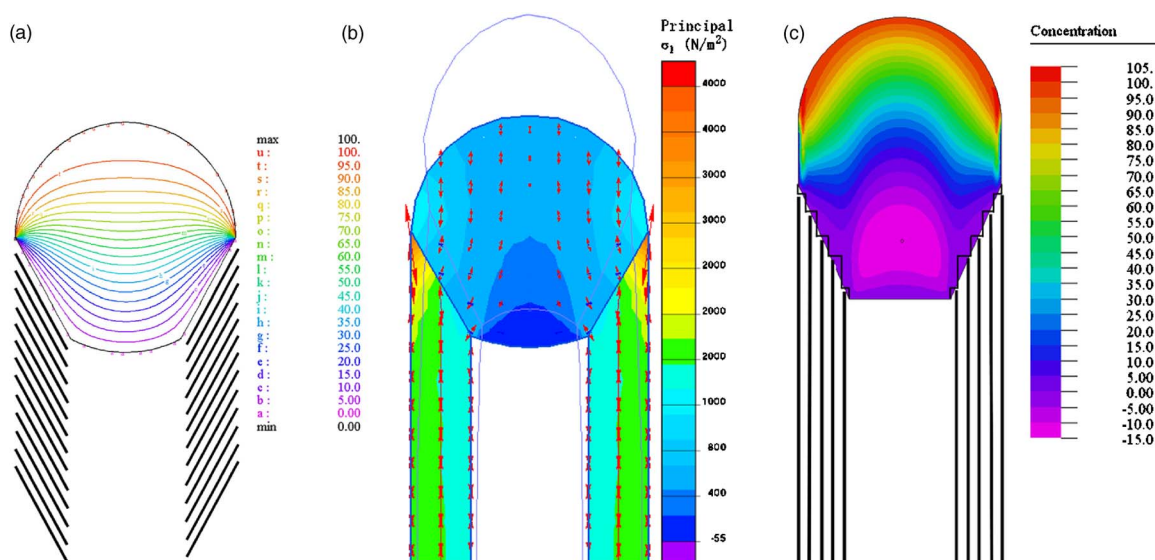


FIG. 4. (Color online) Models for CNT growth: (a) carbon concentration gradient calculated for a conical catalyst particle coupled with the “herringbone” growth model; (b) stress and deformed boundary of the nanotube and the catalyst particle pulled by electrostatic force; (c) carbon concentration gradient calculated for the elongated catalyst particle coupled with the “tubular” growth model.

fusion near the precipitating facets is higher, as shown in Fig. 4(a), which implies that the surface diffusion and bulk diffusion on/in the particle are comparable, and then, the graphite layers precipitate along the conical facets to form a herringbone structure.¹⁸ However, when an electric field is applied, a strong electrostatic force acts upon the particle due to field enhancement which leads to particle elongation, as shown in Fig. 4(b). Then, the surface diffusion becomes prominent and the bulk diffusion becomes negligible because of the tensile stress gradient,^{24,25} as shown in Fig. 4(c). Furthermore, the carbon concentration gradient in the particle suggests that CNT grown from an elongated particle has a larger proportion of carbon assembling in the outer shells.¹⁵ In addition, the electrostatic force induced deformation for the particle results in many active dislocation steps¹⁷ upon the nanoparticle surface which will also adsorb surface-diffused carbon and nucleated graphite layers parallel to the tube axis.

In conclusion, it was verified that the CNT microstructural transformation from the “herringbone” into highly crystalline “tubular” structure can be achieved by adding an external electric field.

This work was supported by the Foundation for the Author of National Excellent Doctoral Dissertation of P. R. China (FANEDD) (No. 200233).

¹R. H. Baughman, A. A. Zakhidov, and W. A. de Heer, *Science* **297**, 787 (2002).

²M. B. Nardelli, J.-L. Fattebert, D. Orlikowski, C. Roland, Q. Zhao, and J. Bernholc, *Carbon* **38**, 1703 (2000).

³J. W. Park, J. Kim, J.-O. Lee, K. C. Kang, J.-J. Kim, and K.-H. Yoo, *Appl. Phys. Lett.* **80**, 133 (2002).

⁴Y. Chen, D. T. Shaw, and L. Guo, *Appl. Phys. Lett.* **76**, 2469 (2000).

⁵S. H. Jo, D. Z. Wang, J. Y. Huang, W. Z. Li, K. Kempa, and Z. F. Ren, *Appl. Phys. Lett.* **85**, 810 (2004).

⁶Y. Chen, D. T. Shaw, X. D. Bai, E. G. Wang, C. Lund, W. M. Lu, and D. D. L. Chung, *Appl. Phys. Lett.* **78**, 2128 (2001).

⁷Y. Y. Wang, S. Gupta, R. J. Nemanich, Z. J. Liu, and L. C. Qin, *J. Appl. Phys.* **98**, 014312 (2005).

⁸C. Ducati, I. Alexandrou, M. Chhowalla, G. A. J. Amaratunga, and J. Robertson, *J. Appl. Phys.* **92**, 3299 (2002).

⁹M. Endo, Y. A. Kim, Y. Fukai, T. Hayashi, M. Terrones, H. Terrones, and M. S. Dresselhaus, *Appl. Phys. Lett.* **79**, 1531 (2001).

¹⁰J. Menda, B. Ulmen, L. K. Vanga, V. K. Kayastha, Y. K. Yap, Z. Pan, I. N. Ivanov, A. A. Puzos, and D. B. Geohegan, *Appl. Phys. Lett.* **87**, 173106 (2005).

¹¹C. Pan, Y. Liu, F. Cao, J. Wang, and Y. Ren, *Micron* **35**, 461 (2004).

¹²Q. Bao and C. Pan, *Nanotechnology* **17**, 1016 (2006).

¹³G. Vitali, M. Rossi, M. L. Terranova, and V. Sessa, *J. Appl. Phys.* **77**, 4307 (1995).

¹⁴D. G. McCulloch, S. Praver, and A. Hoffman, *Phys. Rev. B* **50**, 5905 (1994).

¹⁵C. Ducati, I. Alexandrou, M. Chhowalla, J. Robertson, and G. A. J. Amaratunga, *J. Appl. Phys.* **95**, 6387 (2004).

¹⁶K. Liu, K. Jiang, C. Feng, Z. Chen, and S. Fan, *Carbon* **43**, 2850 (2005).

¹⁷S. Helveg, C. López-Cartes, J. Sehested, P. L. Hansen, B. S. Clausen, J. R. Rostrup-Nielsen, F. Abild-Pedersen, and J. K. Nørskov, *Nature (London)* **427**, 426 (2004).

¹⁸M. Okai, T. Muneyoshi, T. Yaguchi, and S. Sasaki, *Appl. Phys. Lett.* **21**, 3468 (2000).

¹⁹R. T. K. Baker, P. S. Harris, R. B. Thomas, and R. J. Waite, *J. Catal.* **30**, 86 (1973).

²⁰R. T. K. Baker, *Carbon* **27**, 315 (1989).

²¹O. A. Louchev, Y. Sato, and H. Kanda, *Appl. Phys. Lett.* **80**, 2752 (2002).

²²L. H. Liang, F. Liu, D. X. Shi, W. M. Liu, X. C. Xie, and H. J. Gao, *Phys. Rev. B* **72**, 035453 (2005).

²³A. Pantano, M. C. Boyce, and D. M. Parks, *Phys. Rev. Lett.* **91**, 145504 (2003).

²⁴Y. Todokoro and I. Teramoto, *J. Appl. Phys.* **49**, 3527 (1978).

²⁵M. Laudon, N. N. Carlson, M. P. Masquelier, M. S. Daw, and W. Windl, *Appl. Phys. Lett.* **78**, 210 (2001).